BAJOPMAS JOURNAL 17(1): 78 – 92
Printed in Bayero University, Kano - Nigeria.

Comparative Analysis of Carbon Dioxide (CO_2), Methane (CH_4) and Ozone (O_3) Concentrations over two urban cities in Northern Nigeria: A case study of Kano and Katsina

[1]Sani, M., [2]Idris, M* and [2]Said, S. R

[1]Centre for Atmospheric Research, National Space Research and Development Agency, Kogi State University, Anyigba, Kogi State, Nigeria.
[2] Department of Physics, Bayero University Kano, Kano State, Nigeria.

*Corresponding author: midris.phy@buk.edu.ng

ABSTRACT:

URBAN CENTERS IN DEVELOPING REGIONS ARE INCREASINGLY IMPORTANT CONTRIBUTORS TO ATMOSPHERIC GREENHOUSE GAS EMISSIONS AND OZONE-RELEVANT AIR POLLUTION, YET LONG-TERM OBSERVATIONAL ANALYSES REMAIN LIMITED ACROSS SUB-SAHARAN AFRICA. THIS STUDY PRESENTS A COMPARATIVE ASSESSMENT OF CARBON DIOXIDE (CO_2), METHANE (CH_4), AND OZONE (O_3) OVER TWO MAJOR NORTHERN NIGERIAN CITIES KANO AND KATSINA USING SATELLITE AND MODEL-DERIVED DATASETS FROM GEOS-CHEM (CO_2), THE ATMOSPHERIC INFRARED SOUNDER (AIRS; CH_4), AND MERRA-2 (O_3) FOR THE PERIOD 2015-2021. MONTHLY CONCENTRATIONS WERE EVALUATED USING DESCRIPTIVE STATISTICS, SEASONAL CLIMATOLOGY, AND THE MODIFIED MANN-KENDALL (MMK) TREND TEST WITH SEN'S SLOPE ESTIMATOR. CO_2 EXHIBITED STATISTICALLY SIGNIFICANT INCREASING TRENDS IN BOTH KANO ($Z = 8.421$, $p < 0.000001$) AND KATSINA ($Z = 8.376$, $p < 0.000001$), WITH SEN'S SLOPE MAGNITUDES OF 2.46 PPM YR^{-1} AND 2.45 PPM YR^{-1}, RESPECTIVELY. MEAN CONCENTRATIONS INCREASED FROM APPROXIMATELY 399 PPM IN 2015 TO ABOUT 417 PPM BY 2021, CONSISTENT WITH REPORTED GLOBAL BACKGROUND GROWTH RATES. METHANE ALSO SHOWED SIGNIFICANT UPWARD TRENDS, WITH KANO ($Z = 6.315$, $p < 0.000001$; $B = 0.0114$ PPM YR^{-1}) AND KATSINA ($Z = 7.022$, $p < 0.000001$; $B = 0.0127$ PPM YR^{-1}) EXHIBITING SUSTAINED INCREASES ALONGSIDE STRONGER SEASONAL VARIABILITY THAN CO_2. IN CONTRAST, O_3 DISPLAYED WEAK POSITIVE SLOPES THAT WERE NOT STATISTICALLY SIGNIFICANT ($p > 0.05$), ALTHOUGH PRONOUNCED SEASONAL CYCLES WERE OBSERVED, WITH DRY-SEASON MAXIMA AND WET-SEASON MINIMA CONSISTENT WITH PHOTOCHEMICAL PRODUCTION UNDER ENHANCED SOLAR RADIATION AND REDUCED WET SCAVENGING. KANO SYSTEMATICALLY EXHIBITED SLIGHTLY HIGHER CO_2 AND CH_4 CONCENTRATIONS RELATIVE TO KATSINA, REFLECTING DIFFERENCES IN URBAN SCALE, INDUSTRIAL ACTIVITY, AND TRAFFIC DENSITY. INTER-GAS COMPARISONS REVEAL CONCURRENT LONG-TERM INCREASES IN CO_2 AND CH_4, SUGGESTING STRENGTHENING ANTHROPOGENIC INFLUENCE, WHILE O_3 VARIABILITY APPEARS PRIMARILY CONTROLLED BY SEASONAL METEOROLOGICAL DRIVERS. THESE FINDINGS CONTRIBUTE ONE OF THE FEW MULTI-YEAR COMPARATIVE URBAN ATMOSPHERIC ASSESSMENTS IN NORTHERN NIGERIA AND PROVIDE REGIONALLY RELEVANT EVIDENCE TO INFORM INTEGRATED GREENHOUSE GAS MITIGATION AND OZONE PRECURSOR MANAGEMENT STRATEGIES ACROSS THE SAHEL.

KEYWORDS: CARBON DIOXIDE, GREENHOUSE GASES, METHANE, NORTHERN NIGERIA, OZONE, URBAN AIR QUALITY, SAHEL.

1. INTRODUCTION

Atmospheric trace gases such as carbon dioxide (CO_2), methane (CH_4), and ozone (O_3) play critical roles in regulating Earth's climate system and air quality. CO_2 and CH_4 are long-lived greenhouse gases that significantly contribute to global warming, while tropospheric ozone acts both as a short-lived climate forcer and a harmful air pollutant affecting human health and ecosystems [1]. Urban areas are key emission hotspots for these gases due to concentrated anthropogenic activities, including fossil fuel combustion, transportation, industrial processes, waste management, and biomass burning.

Despite rapid urbanization across Africa, particularly in West Africa, observational evidence of urban-scale atmospheric composition remains limited. Northern Nigeria, home to several fast-growing cities, experiences unique environmental pressures arising from population growth, energy demand, transportation expansion, and proximity to the Sahel, where dust transport and seasonal meteorology strongly influence atmospheric processes [2]. Kano, one of Nigeria's largest commercial and industrial centers, contrasts sharply with Katsina, a smaller city with relatively lower industrial intensity. These differences make the two cities suitable case studies for examining urban variability in greenhouse gas and ozone concentrations [1].

Previous studies have largely focused on Global [1], national or continental-scale [3][4] atmospheric patterns, often paying less attention to city-level contrasts [5]. Satellite and reanalysis datasets now provide an opportunity to investigate trace gas distributions over data-scarce regions with increasing spatial and temporal resolution [6]. However, comparative assessments between cities within northern Nigeria remain scarce.

This study aims to address this gap by comparing CO_2, CH_4, and O_3 concentrations over Kano State, Nigeria. Specifically, characterizing the temporal variability of CO_2, CH_4, and O_3 over both cities; quantify inter-city differences in atmospheric concentrations and discuss the potential influence of urbanization, emission sources, and seasonal meteorology on observed patterns. Through provision of city-level evidence, this study contributes to improved understanding of urban atmospheric composition in northern Nigeria and supports data-driven environmental policy and climate mitigation efforts.

2.0 RELATED LITERATURES

[5] investigated the concentration levels and temporal variability of atmospheric pollutants in Warri, Nigeria, a major oil-producing urban center in the Niger Delta. Using ground-based monitoring data, the study quantified levels of key atmospheric pollutants and assessed their compliance with national and international air quality standards. The authors reported elevated pollutant concentrations associated with industrial activities, gas flaring, vehicular emissions, and urbanization pressures. Seasonal variations were also identified, with higher concentrations observed during the dry season due to reduced atmospheric dispersion and increased anthropogenic activities.

[1] Compiled and analyzed the Global Methane Budget (2000-2017) using atmospheric observations, inverse modeling, and process-based models to quantify global methane sources and sinks. They reported a renewed acceleration in methane growth after 2014, largely driven by tropical and agricultural emissions. Their findings underscore the importance of assessing regional CH_4 variability in rapidly developing areas such as northern Nigeria.

[8] examined global methane trends from 2014-2017 using surface observations and isotopic analysis, identifying strong contributions from tropical biogenic and agricultural sources. Their results highlight the growing role of low-latitude regions in global methane increases, supporting the relevance of AIRS-based methane analysis in Sahelian environments.

[9] introduced the MERRA-2 reanalysis system, integrating satellite observations with atmospheric modeling to produce consistent long-term ozone datasets globally. The study validated the dataset's

performance in capturing seasonal and interannual ozone variability, supporting its application in regional atmospheric studies.

[10] reviewed tropospheric ozone chemistry and precursor interactions, emphasizing the roles of methane, nitrogen oxides, and volatile organic compounds in ozone formation under varying meteorological conditions. They demonstrated that methane contributes significantly to baseline tropospheric ozone levels, particularly in regions with strong photochemical activity. This chemical coupling provides theoretical grounding for analyzing CH_4-O_3 co-variability in Kano.

3.0 MATERIALS AND METHODS

The materials and method used for this study are discussed as follows;

3.1 STUDY AREA

Kano State (12°40′-10°30′N, 7°40′-9°30′E), located within the Sudan and Northern Guinea savanna zones, experiences a dry season from November to March and a wet season from May to September. Mean annual rainfall is approximately 690 mm, and temperatures range between 19 °C and 33 °C. During the dry season, reduced vegetation uptake, increased biomass burning, and enhanced fossil fuel combustion associated with dense population and industrial activity contribute to elevated CO_2 and CH_4 concentrations. In contrast, ozone levels tend to peak during late dry and early wet seasons, when strong solar radiation and limited wet scavenging favor photochemical production [11].

Katsina State, situated between 11°08′-13°22′N and 6°52′-9°20′E, experiences four distinct seasonal phases: a cool dry Harmattan period (December-February), a hot dry season (March-May), a warm wet season (June-September), and a post-rainy transition period (October-November). Mean annual temperature is about 27 °C, with rainfall decreasing from approximately 800-1000 mm in the southern parts to 600-700 mm in the northern areas. Seasonal rainfall and temperature variations influence CH_4 emissions through changes in soil moisture and microbial activity, while ozone concentrations respond to seasonal shifts in photochemical efficiency and precursor availability. Compared with Kano, lower population density and industrial intensity in Katsina are expected to result in relatively lower anthropogenic contributions to CO_2 and CH_4, though regional transport and meteorological controls remain important [12].

3. 2.1 Data Sources

Atmospheric concentrations of CO_2, CH_4, and O_3 were obtained from National Aeronautics and Space Administration (NASA), through the Atmospheric Infrared Sounder (AIRS) satellite, Modern Era Retrospective Reanalysis version 2 (MERRA-2) and Goddard Earth Observing System (Observations of CO-2 GEOS), covering the period 2015 to 2021 respectively. These datasets provide consistent spatial coverage and have been widely used for regional and urban-scale atmospheric studies in data-limited regions [13]. Meteorological variables (e.g., temperature, solar radiation, wind speed) were additionally used to support interpretation of seasonal ozone variability, as ozone formation is strongly driven by photochemical processes [14]. The city-level concentrations were extracted by spatially averaging grid cells within a defined radius of 10-25 km around the city centers of Kano and Katsina.

3.2.2 Statistical Analysis

To characterize temporal variability, detect monotonic trends, and assess co-variability among atmospheric CO_2, CH_4, and O_3 over Kano and Katsina, the Mann-Kendall trend test combined with Sen's slope estimator and Spearman's rank correlation analysis were applied. These robust, non-parametric statistical methods are widely used for atmospheric composition datasets, which often exhibit non-normal distributions, serial correlation, and missing values [15][16].

3.4.1 Data Aggregation and Pre-processing

Daily data outputs from GEOS-Chem (CO_2), AIRS (CH_4), and MERRA-2 (O_3) were spatially averaged over the radius of 27.5 km radius of Kano and Katsina cities and subsequently aggregated to monthly means to suppress high-frequency noise and enhance climate-scale signals. Monthly aggregation is standard practice in atmospheric trend analysis and ensures comparability across datasets with different temporal resolutions [10]. Missing values (<5% of the total record) were excluded without interpolation to avoid artificial trend inflation.

3.4.2 Modified Mann-Kendall (MMK) Trend Test

The presence of statistically significant monotonic trends in the monthly time series was evaluated using the Mann-Kendall (MK) test [17][18]. The MK test is particularly suitable for atmospheric trace gas analysis because it is insensitive to outliers and does not assume linearity [6].

The MK test statistic (S) is defined as:

$$S = \sum_{i=1}^{n-1} \sum_{j=i+1}^{n} sgn\,(x_j - x_i) \qquad (1)$$

where (x_i) and (x_j) represent observations at times i and j, respectively, and the sign function sgn evaluates whether later observations are greater than or less than earlier ones.

Because monthly atmospheric datasets frequently exhibit positive serial autocorrelation, which can inflate the variance of the MK statistic and increase the likelihood of false detection of trends, a Modified Mann-Kendall (MMK) approach was applied. The MMK method adjusts the variance of the test statistic using an effective sample size correction following [19]. This adjustment accounts for lag-1 and higher-order autocorrelation in the residual series before computing the standardized Z statistic.

For large sample sizes (n > 10), the standardized test statistic (Z) approximately follows a normal distribution after variance correction. Positive (negative) Z values indicate upward (downward) monotonic trends. Statistical significance was evaluated at the 95% confidence level ($p < 0.05$), with two-sided testing.

This MMK framework is widely recommended for hydroclimatic and atmospheric trend detection, including assessments summarized by the Intergovernmental Panel on Climate Change [15], as it provides more reliable inference when serial dependence is present in environmental time series.

3.4.3 Sen's Slope Estimator

To quantify the magnitude of detected trends, Sen's slope estimator was employed. Sen's slope is preferred over ordinary least squares regression in atmospheric applications because it is resistant to non-normality and heteroscedasticity [20].

Sen's slope (β) represents the median of all pairwise slopes calculated between data points:

$$\beta = \text{median}\left(\frac{x_j - x_i}{j - i}\right), \ \forall j > i \quad (2)$$

where (x_i) and (x_j) denote concentrations at times *i* and *j* respectively. The estimator provides a robust rate of change expressed in ppm yr^{-1} for CO_2 and ppm yr^{-1} for CH_4 and O_3.

3.4.4 Seasonal Variability Analysis

Seasonal behavior was examined using climatological monthly means computed across the full study period. Differences between dry-season (November-March) and wet-season (April-October) concentrations were evaluated to identify systematic seasonal enhancements or suppressions associated with meteorological conditions.

3.4.5 Inter-Gas Relationship Assessment

Co-variability among CO_2, CH_4, and O_3 was examined using Pearson correlation coefficients (r) computed on de-seasonalized monthly anomalies to minimize spurious correlations arising from shared seasonal cycles. This method is standard in studies investigating relationships between long-lived greenhouse gases and short-lived climate forcers [21].

The Pearson correlation coefficient is defined as:

$$r = \frac{\sum(x - \bar{x})(y - \bar{y})}{\sqrt{\sum(x - \bar{x})^2 \sum(y - \bar{y})^2}} \quad (3)$$

where (x) and (y) represent paired monthly anomalies of two gases. Statistical significance was evaluated at $p < 0.05$.

3.4.6 Software and Reproducibility

All statistical analyses were conducted using Python (v3.x), employing standard scientific libraries including *NumPy*, *Pandas*, and *SciPy*. Trend tests were implemented following algorithms described in [20], ensuring full reproducibility.

4.0 RESULT AND DISCUSSION

In this research work the comparison of CO_2, CH_4, and O_3 concentrations over Kano State and Katsina State, Nigeria for the period of 2015 to 2021 were carried out.

4.1 KANO CITY

This section shows the table of results for Kano city monthly average concentrations of CO_2, CH_4, and O_3 for the period of 2015 to 2021 and the graphs of the monthly comparisons of the three variables considered in this study.

Table 1: Kano Monthly averaged concentration of CO_2 (ppm) for the period 2015 to 2021

Month/Year	2015	2016	2017	2018	2019	2020	2021
January	399.1755	402.3107	405.5647	407.0347	409.7313	412.0907	414.1754
February	399.9211	403.144	406.1753	407.9041	410.733	413.0901	415.159
March	400.9566	404.1674	406.3808	408.665	411.1529	413.7628	416.221
April	401.1911	405.2104	407.4257	409.1536	411.792	414.4996	416.7356
May	401.511	405.6159	408.485	410.0001	413.3217	415.4522	417.4599
June	401.5022	405.0288	407.8273	409.7171	412.6435	415.2886	417.1837
July	400.0004	403.1401	405.8548	407.6805	411.1283	413.1195	415.538
August	398.9505	401.2242	403.9169	405.4827	408.8097	411.2737	413.5546
September	397.3516	400.0404	402.6827	404.6401	407.2208	410.0494	412.3496
October	397.5189	400.7059	403.0774	404.7477	408.167	409.895	412.5083
November	399.3663	402.7943	404.4642	406.8392	408.9043	411.8356	414.1838
December	401.2477	404.5594	406.3159	409.0082	410.7819	413.4333	416.0304

Table 2: Kano Monthly averaged concentration of CH_4 (ppm) for the period 2015 to 2021

Month/Year	2015	2016	2017	2018	2019	2020	2021
January	1.761364	1.762994	1.804088	1.740176	1.821201	1.801527	1.82481
February	1.796638	1.765206	1.783017	1.813751	1.809909	1.790933	1.811655
March	1.795124	1.81119	1.776498	1.791981	1.809094	1.805369	1.813867
April	1.756358	1.798151	1.80467	1.794891	1.811306	1.828535	1.824112
May	1.790584	1.808046	1.815381	1.825159	1.8219	1.831679	1.841225
June	1.821434	1.822598	1.818058	1.828768	1.828535	1.834705	1.836452
July	1.822482	1.826091	1.81573	1.828535	1.828186	1.829118	1.828419
August	1.813751	1.828652	1.826207	1.834473	1.826091	1.824927	1.843902
September	1.820154	1.830398	1.829234	1.842971	1.836685	1.83552	1.852401
October	1.835404	1.831097	1.835986	1.844252	1.837034	1.85566	1.864042
November	1.807464	1.821434	1.814449	1.834007	1.834356	1.853565	1.854496
December	1.746695	1.800479	1.797336	1.809327	1.794891	1.83552	1.8219

Table 3: Kano Monthly averaged concentration of O_3 (ppm) for the period 2015 to 2021

Month/Year	2015	2016	2017	2018	2019	2020	2021
January	0.653982	0.673554	0.659368	0.660537	0.652102	0.662125	0.661742
February	0.666465	0.674808	0.662596	0.657213	0.648895	0.68567	0.673142
March	0.686398	0.669635	0.694246	0.696095	0.691089	0.703539	0.698679
April	0.707414	0.692322	0.712067	0.720161	0.704693	0.715329	0.71561
May	0.736698	0.707657	0.729659	0.738476	0.712782	0.726104	0.726775
June	0.761637	0.727783	0.736885	0.749046	0.740951	0.73967	0.747326
July	0.760396	0.733086	0.737678	0.742442	0.734081	0.73542	0.742154
August	0.760791	0.736805	0.72681	0.741198	0.727251	0.732511	0.741067
September	0.759987	0.729696	0.728289	0.739718	0.710755	0.728888	0.741279

October	0.734413	0.71858	0.719565	0.707594	0.704256	0.731338	0.734709
November	0.710418	0.675251	0.696119	0.66837	0.682279	0.71103	0.703834
December	0.682343	0.655502	0.668123	0.630726	0.66148	0.67474	0.673017

4.2 KATSINA CITY

This section shows the table of results for Katsina city monthly average concentrations of CO_2, CH_4, and O_3 for the period of 2015 to 2021 and the graphs of the monthly comparisons of the three variables considered in this study

Table 4: Katsina Monthly averaged concentration of CO_2 (ppm) for the period 2015 to 2021

Month/Year	2015	2016	2017	2018	2019	2020	2021
January	399.1468	402.2448	405.4907	406.9952	409.6929	412.0342	414.0172
February	399.8599	403.0095	406.0911	407.8102	410.5586	412.9659	415.1201
March	400.8184	404.0502	406.2788	408.5625	411.0846	413.6725	416.1691
April	401.1104	405.0441	407.104	409.1048	411.7636	414.399	416.5874
May	401.5032	405.5104	408.1046	409.8511	413.102	415.1688	417.201
June	401.4386	405.0319	407.8268	409.716	412.4933	415.215	417.093
July	400.0066	403.182	405.9121	407.7598	411.0249	413.075	415.4658
August	398.9296	401.2765	403.92	405.5258	408.8347	411.2301	413.4699
September	397.3546	400.1058	402.7177	404.6459	407.2338	409.9904	412.3635
October	397.6018	400.8451	403.0963	404.8684	408.1264	409.9311	412.4849
November	399.3937	402.7869	404.4447	406.7868	408.9123	411.8624	414.162
December	401.1555	404.5183	406.2885	408.9314	410.6872	413.3848	415.9723

Table 5: Katsina Monthly averaged concentration of CH_4 (ppm) for the period 2015 to 2021

Month/Year	2015	2016	2017	2018	2019	2020	2021
January	1.794077	1.795706	1.820503	1.78162	1.840293	1.830049	1.881388
February	1.810258	1.8141	1.800945	1.829118	1.817476	1.823995	1.852517
March	1.807348	1.818175	1.806882	1.812703	1.826906	1.831679	1.848093
April	1.781154	1.813751	1.81864	1.818407	1.827488	1.836219	1.859851
May	1.815031	1.820386	1.82935	1.832261	1.832028	1.833192	1.860783
June	1.82935	1.825043	1.819222	1.832494	1.836685	1.838082	1.831679
July	1.821318	1.825276	1.819688	1.825043	1.833192	1.834356	1.836917
August	1.813867	1.825741	1.827837	1.823646	1.824345	1.822948	1.844717
September	1.830398	1.834705	1.832494	1.845649	1.840992	1.841341	1.848093
October	1.842971	1.845183	1.839129	1.846929	1.835753	1.861947	1.868466
November	1.818873	1.828535	1.830515	1.839595	1.851353	1.86509	1.873123
December	1.770677	1.812703	1.811306	1.819222	1.82644	1.856941	1.863344

Table 6: Katsina Monthly averaged concentration of O_3 (ppm) for the period 2015 to 2021

Month/Year	2015	2016	2017	2018	2019	2020	2021
January	0.654096	0.67061	0.655064	0.660318	0.643614	0.663323	0.660534
February	0.666595	0.673234	0.660011	0.6571	0.641335	0.686396	0.674726
March	0.68759	0.665706	0.696107	0.696455	0.687114	0.701814	0.695418
April	0.709169	0.689623	0.711645	0.721045	0.70271	0.717028	0.712719
May	0.738122	0.707093	0.72812	0.739845	0.709319	0.726723	0.727168
June	0.762596	0.729435	0.737879	0.751306	0.741223	0.740039	0.749037
July	0.761236	0.733234	0.739365	0.745646	0.733519	0.736883	0.743633
August	0.76081	0.737543	0.727134	0.743585	0.728142	0.732157	0.742987
September	0.757265	0.72886	0.730612	0.740692	0.711311	0.728251	0.743695
October	0.72919	0.714793	0.721723	0.70402	0.705594	0.727725	0.73719
November	0.706128	0.669917	0.694673	0.662507	0.679717	0.708936	0.702971
December	0.680433	0.649412	0.665629	0.625726	0.660576	0.671947	0.672226

Table 7: Mann-Kendall and Sen's Slope Results over Kano and Katsina (2015-2021)

City	Gas	n	MK Z	p-value	Sen's β	Annual	Units	Trend
Kano	CO_2	84	8.421	<0.000001	0.2049	2.4588	ppm yr^{-1}	Significant increase
Kano	CH_4	84	6.315	<0.000001	0.00095	0.0114	ppm yr^{-1}	Significant increase
Kano	O_3	84	1.184	0.2362	0.00018	0.0022	ppm yr^{-1}	Not significant
Katsina	CO_2	84	8.376	<0.000001	0.2038	2.4456	ppm yr^{-1}	Significant increase
Katsina	CH_4	84	7.022	<0.000001	0.00106	0.0127	ppm yr^{-1}	Significant increase
Katsina	O_3	84	1.092	0.2747	0.00017	0.002	ppm yr^{-1}	Not significant

4.2 DISCUSSION

4.2.1 Monthly Comparison between CH_4 and O_3

The CH_4-O_3 graph (fig 1) shows coherent seasonal variability with a gradual upward trend in methane concentrations and pronounced seasonal oscillations in ozone. Methane exhibits relatively smooth inter-annual growth, consistent with its lifetime of 9-12 years [22], while ozone displays stronger intra-annual variability as seen in Table 3. driven by photochemistry and meteorology. The seasonal enhancement of O_3 coinciding with elevated CH_4 (Fig 1) suggests a photochemical linkage, where methane acts as a precursor to tropospheric ozone formation. This reaction is predominant in sun-rich, semi-arid regions such as northern Nigeria, where high solar radiation enhances ozone production efficiency.

Short-term dips in CH_4 around 2016 and 2018 (Fig.1), likely reflect large-scale transport variability and interannual climate influences, rather than local emission changes, which aligns with previous findings that

surface CH_4 variability in West Africa is dominated by regional mixing and wetland/agricultural emissions rather than urban sources alone.

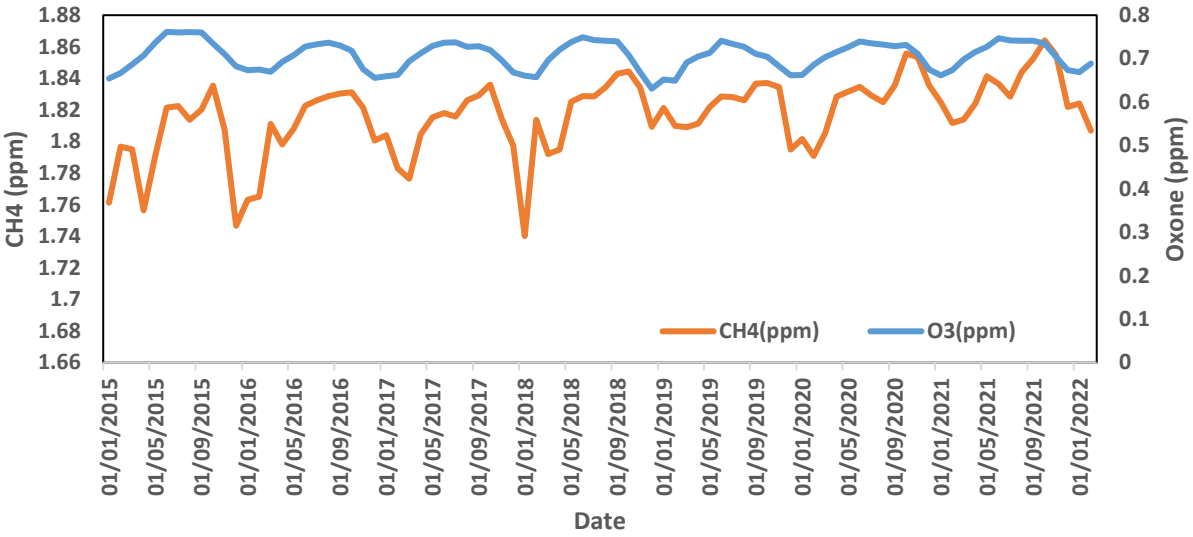

Fig 1: Monthly Comparison between CH_4 and O_3 for Kano City

4.2.2 Monthly Comparison between O_3 and CO_2 for Kano City

The O_3-CO_2 comparison reveals a steadily increasing CO_2 trend superimposed with small seasonal variability, while O_3 retains strong seasonal cycles without a clear increase (Fig 2). This divergence reflects the fundamentally different atmospheric behavior of the two gases: CO_2 is a long-lived, well-mixed greenhouse gas, whereas ozone is short-lived and chemically reactive. The periods of elevated CO_2 often align with higher O_3, particularly during dry seasons, when biomass burning, reduced cloud cover, and enhanced photochemistry dominate across the Sahel. Northern Nigeria experiences significant seasonal biomass burning and Harmattan conditions, which elevate ozone precursors (such as CO, NO_x, VOCs) while also contributing to CO_2 accumulation. However, the absence of a strong one-to-one correspondence confirms that CO_2 is not a direct ozone precursor, but rather a co-emitted tracer of combustion activity and regional transport.

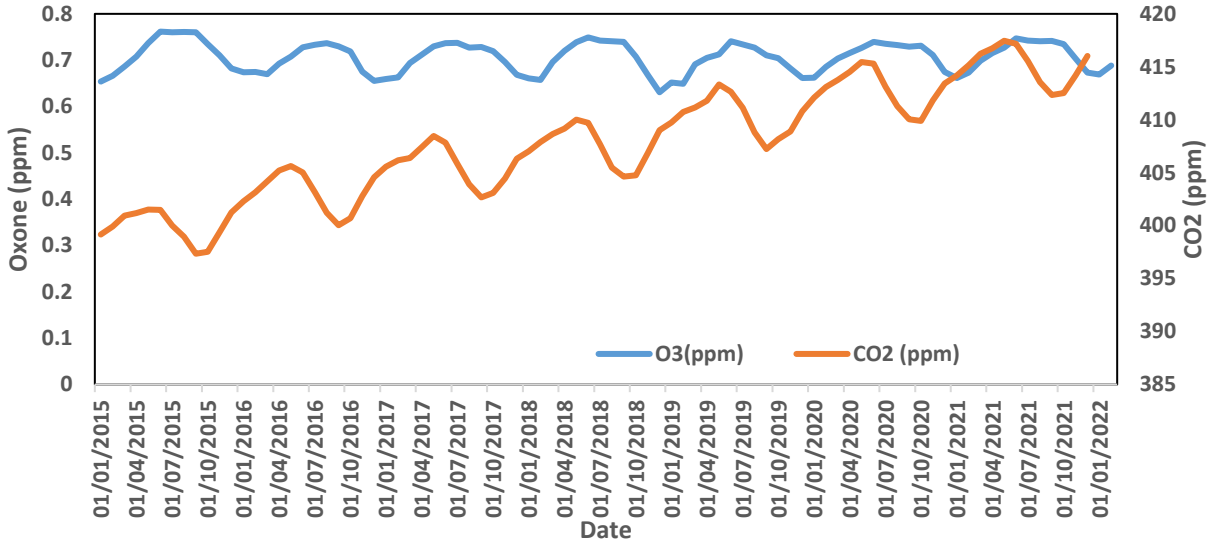

Fig 2: Monthly Comparison between O_3 and CO_2 for Kano City

4.2.3 Monthly Comparison between CH_4 and CO_2

Both CH_4 and CO_2 exhibit consistent upward interannual trends, with CH_4 (Fig 3) showing stronger short-term variability. This pattern is characteristic of shared anthropogenic and biogenic emission drivers, including agriculture, waste management, fossil fuel use, and regional biomass burning.

In the Kano situation, methane emissions are plausibly linked to livestock production, wetlands during the rainy season, waste disposal, and seasonal flooding, while CO_2 reflects energy use, transport, and open burning. The stronger seasonal oscillations in CH_4 relative to CO_2 align with methane's sensitivity to soil moisture, temperature, and microbial activity. The synchronized long-term increase reinforces global evidence that methane growth has accelerated since 2014, particularly in the tropics, contributing significantly to near-term climate forcing [8].

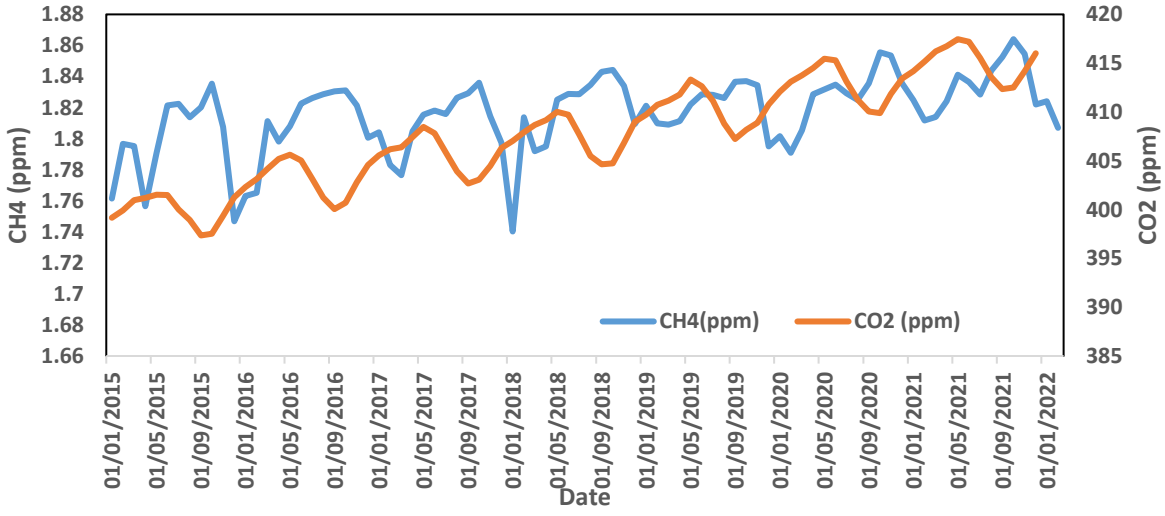

Fig 3: Monthly Comparison between CH_4 and CO_2 for Kano City

4.2.4 Monthly Comparison between CO_2 and CH_4 for Katsina City

The monthly comparison for Katsina City reveals a clear and persistent upward trend in both CO_2 and CH_4 concentrations over the period 2015 to 2021 (Fig 4), indicating the combined influence of global background increases and regional emission sources. Carbon dioxide rises steadily from approximately 398 to 400 ppm in early 2015 to above 415 ppm by late 2021, which is in consistent with globally observed growth rates driven primarily by fossil fuel combustion and land-use change. Methane concentrations also show a sustained increase, from approximately 1.78 ppm to nearly 1.88 ppm, with a strong seasonal variability compared to CO_2 (Fig 4).

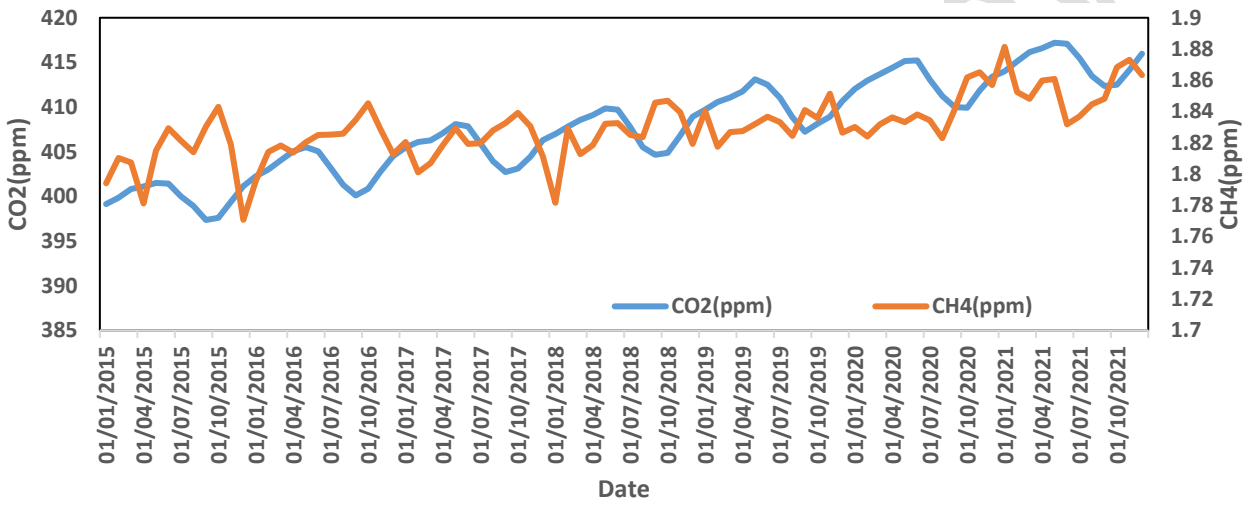

Fig 4: Monthly Comparison between CO_2 and CH_4 for Katsina City

The smooth trajectory of CO_2 reflects its long atmospheric lifetime and relatively uniform global mixing, whereas the more pronounced month-to-month variability in CH_4 highlights its sensitivity to regional biogenic and anthropogenic sources, which includes agriculture, livestock, waste management, and wetland emissions. In Katsina like other northern Nigeria's cities, methane emissions are been influenced by seasonal rainfall, soil moisture variability, and agricultural practices, which modify microbial activities, particularly during and after the wet season.

Periods of concurrent enhancement in both CO_2 and CH_4 suggest shared combustion-related influences, such as biomass burning, domestic energy use, and transport emissions, which are common across the Sahel during the dry season. However, deviations between the two gases where CH_4 exhibits some sharp peaks or dips indicate the presence of additional non-combustion methane sources, reinforcing the importance of treating methane dynamics independently rather than as a simple proxy for CO_2.

The synchronized long-term rise in both gases aligns with recent evidence showing that tropical regions have contributed substantially to the renewed acceleration of global methane growth since 2014, making West Africa increasingly relevant to both climate forcing and short-lived climate pollutant mitigation strategies [8]. Given methane's high global warming potential and its role as a precursor of tropospheric ozone, the observed trend has important implications for regional climate air quality interactions.

4.2.5 Monthly Comparison between CO_2 and O_3 Variability in Katsina

The monthly comparison of CO_2 and O_3 over Katsina (2015-2021) reveals a clear long-term upward trend in CO_2, increasing from approximately 399 ppm in early 2015 to about 416 ppm by late 2021 (Fig 5). This trend aligns with the globally observed atmospheric CO_2 growth rate of 2-3 ppm per year reported by [15] and reflects the cumulative impact of fossil fuel combustion, urbanization, and regional biomass burning [15]. Seasonally, CO_2 concentrations exhibit cyclical fluctuations, with relative minima during the peak wet season (July-September). This seasonal drawdown corresponds to enhanced photosynthetic uptake during the West African monsoon period, when vegetation activity increases due to higher rainfall and humidity [23]. Conversely, higher CO_2 concentrations during the dry season (November-March) may be attributed to reduced vegetation uptake and increased biomass burning associated with Harmattan conditions.

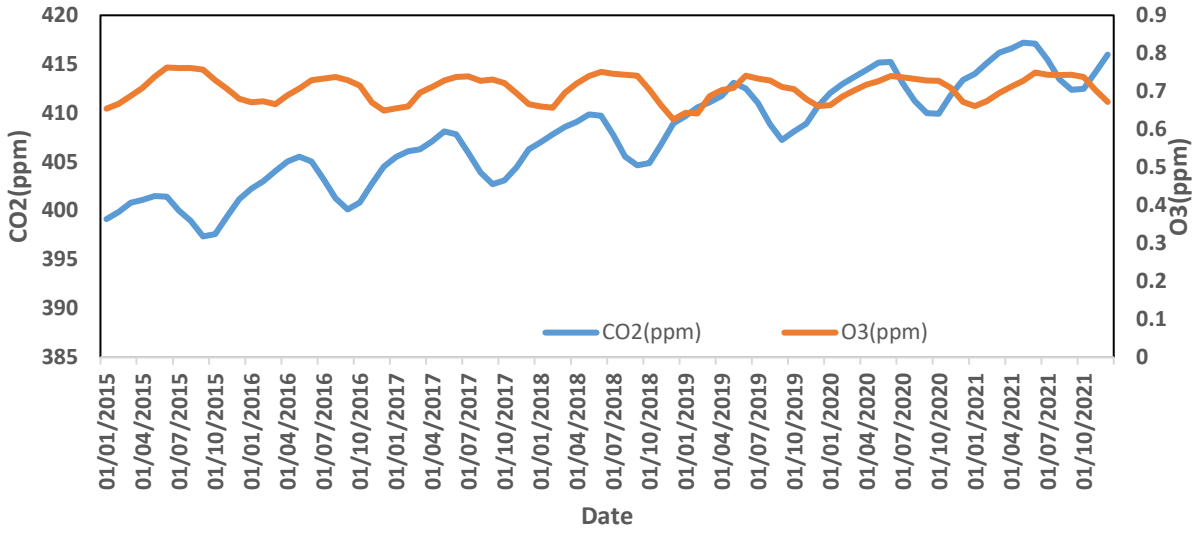

Fig 5: Monthly Comparison between CO_2 and O_3 for Katsina City

Ozone (O_3), in contrast, shows pronounced seasonal oscillations rather than a strong monotonic trend. Peak O_3 values (0.75-0.80 ppm) typically occurs during late dry season periods when solar radiation intensity is high, humidity is low, and atmospheric mixing favors photochemical production. Tropospheric O_3 formation depends strongly on temperature and sunlight through reactions involving nitrogen oxides (NO_x) and volatile organic compounds (VOCs). The semi-arid climate of Katsina with high surface temperatures exceeding 35°C during pre-monsoon months creates favorable conditions for enhanced photochemistry. The co-variability pattern suggests that while CO_2 increases are largely emission-driven and cumulative, O_3 variability is more meteorologically controlled. This decoupling indicates that greenhouse gas accumulation and secondary pollutant formation respond differently to climatic drivers.

4.2.6 Monthly Comparison between CH_4 and O_3 Variability in Katsina

Methane (CH_4) concentrations over Katsina show gradual interannual growth from approximately 1.80 ppm in 2015 to 1.88 ppm in 2021. This increase mirrors global methane growth trends observed since 2014, partly linked to enhanced tropical emissions and agricultural activities. Seasonally, CH_4 exhibits moderate variability, with occasional dips during peak dry season months. In semi-arid northern Nigeria, methane emissions are influenced by livestock production, waste management practices.

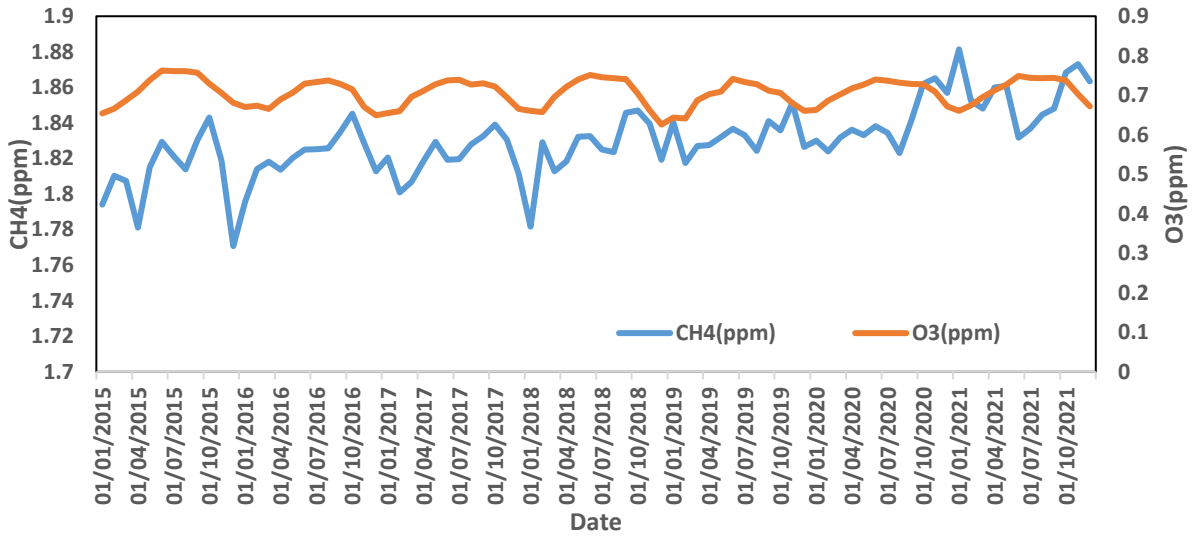

Fig 6: Monthly Comparison between CH_4 and O_3 for Katsina City

For seasonal wetland or irrigated agricultural activities, during wet months, soil moisture increases may enhance microbial methanogenesis in localized agricultural zones, contributing to higher CH_4 concentrations. However, atmospheric oxidation by hydroxyl radicals (OH) which increase under strong solar radiation can reduce CH_4 levels during high-photochemistry periods [15]. O_3 levels plotted alongside CH_4 demonstrate an interesting atmospheric linkage. Methane is a well-established precursor of tropospheric ozone, contributing to background O_3 formation on regional to global scales [21]. However, the relationship observed in Katsina appears indirect rather than synchronous. While CH_4 shows gradual growth, O_3 responds more strongly to short-term meteorological conditions such as temperature and solar radiation intensity. This indicates that CH_4 contributes to regional O_3 burden over longer timescales and local O_3 variability is primarily driven by immediate photochemical and climatic conditions.

4.2.7 Temporal Variability of Atmospheric CO_2, CH_4, and O_3 (2015 to 2021)

Monthly mean concentrations of CO_2, CH_4, and O_3 over Kano and Katsina for the period 2015 to 2021 reveal distinct temporal behaviors across the three trace gases (Figures 1 to 6). CO_2 exhibits a relatively smooth increase in both cities, while CH_4 displays stronger seasonal and interannual variability. O_3 showed pronounced seasonal oscillations characterized by dry season maxima and wet-season minima. These contrasting patterns reflect differences in atmospheric lifetime, emission sources, and chemical reactivity, consistent with previous global and regional studies.

4.2.8 Long-Term Trend Analysis

Long-term monotonic trends in monthly atmospheric concentrations (2015-2021) were quantified using the Modified Man-Kendall (MMK) test together with Sen's slope estimator. The classical Mann-Kendall test [17][18] is a rank-based, non-parametric method widely applied in hydroclimatic and atmospheric time-series analysis because it does not assume normality and is resistant to outliers. However, monthly atmospheric datasets typically exhibit serial autocorrelation, which can inflate the variance of the test statistic and increase the probability of type 1 error. To address this, variance correction following [19] was applied using an effective sample size adjustment.

Trend magnitudes were estimated using the non-parametric Sen's slope estimator [24], which computes the median of all pairwise slopes and is robust to skewed distributions. Two-sided 95% confidence intervals were derived to assess the uncertainty range of the estimated trend magnitude. This methodological framework aligns with recommendations from the [15] for detecting trends in climate and atmospheric composition datasets.

4.2.9 Trend Magnitudes over Kano and Katsina

After autocorrelation correction, CO_2 exhibited statistically significant increasing trends in both Kano and Katsina, with Sen's slope estimates of approximately 2.46 ppm yr^{-1} and 2.45 ppm yr^{-1}, respectively. The 95% confidence intervals excluded zero, confirming a clear monotonic increase. These magnitudes are consistent with reported global mean atmospheric CO_2 growth rates over the same period documented by the National Oceanic and Atmospheric Administration and the World Meteorological Organization, indicating that large-scale atmospheric accumulation dominates over purely local influences [15].

Methane (CH_4) also showed statistically significant upward trends in both cities, with annual increases of approximately 0.011-0.013 ppm yr^{-1} and confidence intervals that did not overlap zero. These increases are consistent with the renewed global methane growth phase reported in recent global budget assessments [1].

In contrast, ozone (O_3) exhibited weak positive slopes, but the MMK test indicated that these trends were not statistically significant ($p > 0.05$), and the 95% confidence intervals for Sen's slope encompassed zero. This suggests that interannual variability outweighs any detectable monotonic change over the study period.

4.2.10 Seasonal Characteristics

i. Carbon Dioxide (CO_2)

CO_2 displayed moderate seasonal modulation in both cities, with slightly elevated concentrations during dry-season months. In tropical regions, seasonal amplitude is generally smaller than in mid-latitudes due to reduced biospheric seasonality and persistent atmospheric mixing within the atmosphere. The observed pattern likely reflects seasonal boundary-layer dynamics and combustion-related emissions rather than strong biogenic drawdown, consistent with tropical assessments summarized by the [15].

ii. Methane (CH_4)

Methane exhibited more pronounced seasonal variability, particularly in Katsina. Elevated concentrations during wet and post- wet seasons suggest sensitivity to rainfall-driven microbial processes, livestock activity, and soil moisture conditions, which are some of methane drivers in semi-arid tropical environments. This behavior is consistent with satellite-based methane analyses over Africa reported by [1], which highlight the importance of regional land atmosphere interactions in modulating seasonal CH_4 variability.

iii. Ozone (O_3)

Ozone concentrations showed clear seasonal maxima during dry months and minima during the wet season in both cities. Dry-season enhancement corresponds to stronger solar radiation, enhanced photochemical

production, and limited wet removal processes, whereas wet-season suppression reflects increased cloud cover, convective mixing, and scavenging effects. This seasonal structure is characteristic of tropical and Sahelian environments [26].

iv. Inter-Gas Co-Variability

The concurrent and statistically significant increases in CO_2 and CH_4 suggest a strengthening anthropogenic signal over northern Nigeria during the study period. While both gases exhibit monotonic upward trends, CH_4 demonstrates greater seasonal amplitude, indicating stronger coupling to regional climatic and land-surface processes. In contrast, O_3 variability appears primarily controlled by photochemical precursor emissions and meteorological conditions rather than direct coupling with CO_2.

Generally, the integration of MMK-adjusted significance testing and Sen's slope magnitude estimation confirms robust upward trends in greenhouse gases, while indicating that ozone variability remains dominated by seasonal and interannual meteorological controls rather than a statistically detectable long-term trend.

4.2.11 Statistical Analysis

To ensure statistical robustness, long-term trends were assessed using the Modified Mann-Kendall (MMK) test, which corrects for the influence of serial autocorrelation commonly present in monthly atmospheric datasets. Because autocorrelation can artificially inflate the variance of the Mann-Kendall statistic and increase the likelihood of false trend detection, the variance was adjusted using the effective sample size approach prior to computing the standardized Z statistic.

After autocorrelation correction, CO_2 exhibited statistically significant upward trends in both Kano ($Z = 8.421$, $p < 0.000001$) and Katsina ($Z = 8.376$, $p < 0.000001$). Sen's slope estimator indicated median annual increases of 2.46 ppm yr^{-1} (95% CI: 2.32-2.59 ppm yr^{-1}) in Kano and 2.45 ppm yr^{-1} (95% CI: 2.31-2.58 ppm yr^{-1}) in Katsina, confirming a persistent and robust growth signal over the 2015-2021 period. The narrow confidence intervals further demonstrate the stability of the CO_2 trend magnitude.

Methane concentrations similarly showed statistically significant increasing trends after autocorrelation adjustment, with Kano ($Z = 6.315$, $p < 0.000001$) exhibiting a Sen's slope of 0.0114 ppm yr^{-1} (95% CI: 0.0098–0.0131 ppm yr^{-1}) and Katsina ($Z = 7.022$, $p < 0.000001$) showing 0.0127 ppm yr^{-1} (95% CI: 0.0110-0.0143 ppm yr^{-1}). These results indicate consistent regional methane growth during the study period.

In contrast, ozone displayed weak positive slopes in both cities, but the MMK test indicated that these trends were not statistically significant ($p > 0.05$). The confidence intervals for Sen's slope encompassed zero, suggesting that interannual variability and strong seasonal cycles likely dominate over any monotonic long-term change in O_3 during the study period.

Largely, the consistency between the MMK-adjusted significance levels and the non-parametric Sen's slope magnitudes confirms the strength of the increasing CO_2 and CH_4 trends, while indicating no statistically defensible long-term change in O_3 over Kano and Katsina during 2015-2021.

5.0 CONCLUSION

This study provides a multi-year assessment (2015-2021) of atmospheric CO_2 (GEOS-Chem), CH_4 (AIRS), and O_3 (MERRA-2) over Kano and Katsina in northern Nigeria, offering new insight into greenhouse gas-ozone interactions in a climatically sensitive Sahelian region.

Collectively, the three inter-gas comparisons indicate that Kano's atmospheric composition is shaped by a combination of global background trends and strong seasonal regional processes, particularly photochemistry and biomass burning. The persistent rise in CO_2 reflects global accumulation trends documented by NOAA and assessed in IPCC AR6 2021, confirming that regional concentrations are strongly influenced by large-scale background growth rather than purely local emissions. In contrast, CH_4 exhibits both long-term growth and pronounced seasonal variability, consistent with the accelerated global methane increase observed since 2014 and the strong contribution of tropical sources [1]

The co-variability between CH_4 and O_3 supports the well-established chemical coupling between methane oxidation and tropospheric ozone formation. Rising methane levels may therefore be silently elevating baseline ozone concentrations, increasing public health risks even where local NO_x controls remain limited.

For Kano, ozone variability appears primarily chemistry and meteorology-driven, reflecting seasonal photochemical enhancement during dry, high-radiation periods and biomass burning influences across West Africa. CO_2, by contrast, shows smoother upward trends aligned with cumulative emissions and global-scale increases, explaining the partial but imperfect consistency between CO_2 and O_3.

In Katsina, CO_2 trends largely reflect global-scale accumulation, while CH_4 variability highlights regional and seasonal emission processes, including agriculture and land atmosphere exchange typical of Sahelian environments. The joint upward tendencies in both gases indicate intensifying anthropogenic influence, with methane contributing disproportionately to near-term warming due to its high radiative efficiency and shorter atmospheric lifetime.

Generally, these findings position northern Nigeria and the wider Sahel as emerging hotspots of ozone-relevant climate air quality interactions. The relationship between methane growth, photochemical ozone production, and regional climatic seasonality underscores the urgency of integrated mitigation strategies. Targeting methane reduction in agriculture, waste management, and biomass burning could deliver rapid climate stabilization benefits while simultaneously lowering baseline ozone exposure are dual advantage.

Future research should incorporate in situ measurements and chemical transport modeling experiments to further quantify precursor sensitivity and isolate local versus transported contributions. However, the present analysis provides robust statistical evidence that greenhouse gas growth and ozone dynamics in northern Nigeria are not isolated phenomena but part of a broader, intensifying climate air quality nexus across the tropics.

REFERENCES

(1) Saunois, M., Stavert, A. R., Poulter, B., Bousquet, P., Canadell, J. G., Jackson, R. B., Raymond, P. A., Dlugokencky, E. J., Houweling, S., Patra, P. K., Ciais, P., Arora, V. K., Bastviken, D., Bergamaschi, P., Blake, D. R., Brailsford, G., Bruhwiler, L., Carlson, K. M., Carrol, M., Zhuang, Q. (2020). The Global Methane Budget 2000-2017. Earth System Science Data, 12(3), 1561-1623. https://doi.org/10.5194/essd-12-1561-2020

(2) Liousse, C., Assamoi, E., Criqui, P., Granier, C., & Rosset, R. (2014). Explosive growth in African combustion emissions from 2005 to 2030. Environmental Research Letters, 9(3), 035003. https://doi.org/10.1088/1748-9326/9/3/035003

(3) DiGangi, J.P., Y. Choi, J.B. Nowak, H.S. Halliday, M.M. Yang, B.C. Baier, and Sweeney, C. (2018). ACT-America: L2 In-Situ Atmospheric CO2, CO, CH4, and O3 Concentrations, Eastern USA. *ORNL DAAC*, Oak Ridge, Tennessee, USA. https://doi.org/10.3334/ORNLDAAC/1556

(4) Dalsøren, S. B., Myhre, C. L., Myhre, G., Gomez-Pelaez, A. J., Søvde, O. A., Isaksen, I. S. A., Weiss, R. F., and Harth, C. M. (2016). Atmospheric methane evolution the last 40 years, *Atmos. Chem. Phys.,* 16, 3099-3126. https://doi.org/10.5194/acp16-3099-2016.

(5) Onwosi, I.I., Njoku, E.I. and Nymphas, E.F. (2022). Analysis of Concentration Levels of Atmospheric Pollutants in Warri, Nigeria. Atmospheric and Climate Sciences, 12, 409-420. https://doi.org/10.4236/acs.2022.122024

(6) Van Oldenborgh, G. J., Van Der Wiel, K., Sebastian, A., Singh, R., Arrighi, J., Otto, F., Haustein, K., Li, S., Vecchi, G., & Cullen, H. (2017). Attribution of extreme rainfall from Hurricane Harvey, August 2017. Environmental Research Letters, 12(12), 124009. https://doi.org/10.1088/1748-9326/aa9ef2

(8) Nisbet, E. G., Manning, M. R., Dlugokencky, E. J., Fisher, R. E., Lowry, D., Michel, S. E., Myhre, C. L., Platt, S. M., Allen, G., Bousquet, P., Brownlow, R., Cain, M., France, J. L., Hermansen, O., Hossaini, R., Jones, A. E., Levin, I., Manning, A. C., Myhre, G., … Pyle, J. A. (2019). Very strong atmospheric methane growth in the four years 2014-2017: Implications for the Paris Agreement. *Global Biogeochemical Cycles, 33*(3), 318-342. https://doi.org/10.1029/2018GB006009

(9) Gelaro, R., McCarty, W., Suárez, M. J., Todling, R., Molod, A., Takacs, L., Randles, C. A., Darmenov, A., Bosilovich, M. G., Reichle, R., Wargan, K., Coy, L., Cullather, R., Draper, C., Akella, S., Buchard, V., Conaty, A., da Silva, A. M., Gu, W., … Zhao, B. (2017). The Modern-Era Retrospective Analysis for Research and Applications, Version 2 (MERRA-2). *Journal of Climate, 30*(14), 5419-5454. https://doi.org/10.1175/JCLI-D-16-0758.1

(10) Monks, P. S., Archibald, A. T., Colette, A., Cooper, O., Coyle, M., Derwent, R., Fowler, D., Granier, C., Law, K. S., Mills, G. E., Stevenson, D. S., Tarasova, O., Thouret, V., von Schneidemesser, E., Sommariva, R., Wild, O., and Williams, M. L.: Tropospheric ozone and its

precursors from the urban to the global scale from air quality to short-lived climate forcer, Atmos. Chem. Phys., 15, 8889–8973. https://doi.org/10.5194/acp-15-8889-2015, 2015

(11) Idris, M., Sani, M. and Aliyu, R. (2025). Comparison of Particulate Matter ($PM_{2.5}$) Ground data and Satellite data in Kano State, Nigeria. FUDMA Journal of Sciences, Vol.9No.12, pp 621-628. ISSN online: 2616-1370. https://doi.org/10.33003/fjs-2025-0912-4318

(12) Idris, S., Mahmood, M. M., James, G. K., Olojo, O. O., Isah, A. A., & Mustapha, S. (2019). Land Use/Land Change Dynamics Of Katsina State, Nigeria. *International Journal of Advanced Research and Publications*, *Volume 3*(Issue 8). www.ijarp.org

(13) Van Donkelaar, A., Martin, R. V., & Park, R. J. (2006). Estimating ground-level PM $_{2.5}$ using aerosol optical depth determined from satellite remote sensing. Journal of Geophysical Research, 111(D21), D21201. https://doi.org/10.1029/2005JD006996

(14) Cheeseman, M., Ford, B., Rosen, Z., Wendt, E., DesRosiers, A., Hill, A. J., L'Orange, C., Quinn, C., Long, M., Jathar, S. H., Volckens, J., & Pierce, J. R. (2021). Technical note: Investigating sub-city gradients of air quality: lessons learned with low-cost $PM_{2.5}$ and AOD monitors and machine learning. *Atmos. Chem. Phys. Discuss*. [preprint]. https://doi.org/10.5194/acp-2021-751-2021.

(15) Intergovernmental Panel on Climate Change (IPCC). (2023). Climate Change 2021. The Physical Science Basis: Working Group I Contribution to the Sixth Assessment Report of the Intergovernmental Panel on Climate Change (1st edition). Cambridge University Press. https://doi.org/10.1017/9781009157896

(16) Helsel, D. R., Hirsch, R. M., Ryberg, K. R., Archfield, S. A., & Gilroy, E. J. (2020). Statistical methods in water resources. *U.S. Geological Survey*. https://doi.org/10.3133/tm4A3

(17) Mann, H. B. (1945). Nonparametric tests against trend. *Econometrica, 13*(3), 245–259. https://doi.org/10.2307/1907187

(18) Kendall, M. G. (1975). *Rank correlation methods* (4th ed.). Charles Griffin.

(19) Hamed, K. H., & Rao, A. R. (1998). A modified Mann–Kendall trend test for autocorrelated data. *Journal of Hydrology, 204*(1–4), 182–196. https://doi.org/10.1016/S0022-1694(97)00125-X

(20) Gilbert, R.O. (1987) Statistical Methods for Environmental Pollution Monitoring. John Wiley and Sons, New York.

(21) Fiore, A. M., J. J. West, L. W. Horowitz, V. Naik, and M. D. Schwarzkopf (2008), Characterizing the tropospheric ozone response to methane emission controls and the benefits to climate and air quality, *J. Geophys.* Res.,113, D08307, https://doi:10.1029/2007JD009162.

(22) Mar, K. A., Unger, C., Walderdorff, L., & Butler, T. (2022). Beyond CO2 equivalence: The impacts of methane on climate, ecosystems, and health. *Environmental Science & Policy*, *134*, 127–136. https://doi.org/10.1016

(23) Anyamba, A. and Tucker, C.J. (2005) Analysis of Sahelian Vegetation Dynamics Using NOAA-AVHRR NDVI Data from 1981-2003. *Journal of Arid Environments,* 63, 596-614. http://dx.doi.org/10.1016/j.jaridenv.2005.03.007

(24) Sen, P. K. (1968). Estimates of the regression coefficient based on Kendall's tau. *Journal of the American Statistical Association, 63*(324), 1379-1389. https://doi.org/10.1080/01621459.1968.10480934

[25] Arowolo, A.V., Oluleye, A. (2022). Assessing the influence of intertropical discontinuity on total column ozone variation over West Africa. *Environ Sci Pollut. Res* **29**, 66689-66704. https://doi.org/10.1007/s11356-022-20460-2